



ELSEVIER

Contents lists available at ScienceDirect

## CYTOTHERAPY

journal homepage: [www.isct-cytotherapy.org](http://www.isct-cytotherapy.org)
 International Society  
**ISCT**  
 Cell & Gene Therapy®

## FULL-LENGTH ARTICLE

## Immunotherapy

# Phospholipid scramblase 1 is involved in immunogenic cell death and contributes to dendritic cell–based vaccine efficiency to elicit antitumor immune response *in vitro*

 Barbara Montico<sup>1,a</sup>, Annunziata Nigro<sup>2,1</sup>, Maria Julia Lamberti<sup>3</sup>, Debora Martorelli<sup>1</sup>,  
 Katy Mastorci<sup>1</sup>, Maria Ravo<sup>4</sup>, Giorgio Giurato<sup>5</sup>, Agostino Steffan<sup>1</sup>, Riccardo Dolcetti<sup>6,7,8,9</sup>,  
 Vincenzo Casolaro<sup>2,\*</sup>, Jessica Dal Col<sup>2,\*\*</sup>
<sup>1</sup> Immunopathology and Cancer Biomarkers, Centro di Riferimento Oncologico di Aviano (CRO), IRCCS, Aviano, Italy<sup>2</sup> Department of Medicine, Surgery and Dentistry 'Scuola Medica Salernitana', University of Salerno, Baronissi, Salerno, Italy<sup>3</sup> Departamento de Biología Molecular, INBIAS, Universidad Nacional de Río Cuarto, Río Cuarto, Córdoba, Argentina<sup>4</sup> Genomix4Life Srl, Baronissi, Salerno, Italy<sup>5</sup> Laboratory of Molecular Medicine and Genomics, Department of Medicine, Surgery and Dentistry "Scuola Medica Salernitana", University of Salerno, Baronissi, Salerno, Italy<sup>6</sup> Centre for Cancer Immunotherapy, Peter MacCallum Cancer Centre, Melbourne, Victoria, Australia<sup>7</sup> Sir Peter MacCallum Department of Oncology, The University of Melbourne, Melbourne, Victoria, Australia<sup>8</sup> Department of Microbiology and Immunology, The University of Melbourne, Melbourne, Victoria, Australia<sup>9</sup> Faculty of Medicine, The University of Queensland Diamantina Institute, Brisbane, Queensland, Australia

## ARTICLE INFO

## Article History:

Received 22 June 2023

Accepted 20 November 2023

Available online xxx

## Key Words:

 DC-based vaccine  
 immunogenic cell death  
 mantle cell lymphoma  
 phospholipid scramblase 1

## ABSTRACT

**Background aims:** Whole tumor cell lysates (TCLs) obtained from cancer cells previously killed by treatments able to promote immunogenic cell death (ICD) can be efficiently used as a source of tumor-associated antigens for the development of highly efficient dendritic cell (DC)-based vaccines. Herein, the potential role of the interferon (IFN)-inducible protein phospholipid scramblase 1 (PLSCR1) in influencing immunogenic features of dying cancer cells and in enhancing DC-based vaccine efficiency was investigated.

**Methods:** PLSCR1 expression was evaluated in different mantle-cell lymphoma (MCL) cell lines following ICD induction by 9-cis-retinoic acid (RA)/IFN- $\alpha$  combination, and commercial kinase inhibitor was used to identify the signaling pathway involved in its upregulation. A Mino cell line ectopically expressing PLSCR1 was generated to investigate the potential involvement of this protein in modulating ICD features. Whole TCLs obtained from Mino overexpressing PLSCR1 were used for DC loading, and loaded DCs were employed for generation of tumor antigen-specific cytotoxic T lymphocytes.

**Results:** The ICD inducer RA/IFN- $\alpha$  combination promoted PLSCR1 expression through STAT1 activation. PLSCR1 upregulation favored pro-apoptotic effects of RA/IFN- $\alpha$  treatment and enhanced the exposure of calreticulin on cell surface. Moreover, DCs loaded with TCLs obtained from Mino ectopically expressing PLSCR1 elicited *in vitro* greater T-cell-mediated antitumor responses compared with DCs loaded with TCLs derived from Mino infected with empty vector or the parental cell line. Conversely, PLSCR1 knock-down inhibited the stimulating activity of DCs loaded with RA/IFN- $\alpha$ -treated TCLs to elicit cyclin D1 peptide-specific cytotoxic T lymphocytes.

**Conclusions:** Our results indicate that PLSCR1 improved ICD-associated calreticulin exposure induced by RA/IFN- $\alpha$  and was clearly involved in DC-based vaccine efficiency as well, suggesting a potential contribution in the control of pathways associated to DC activation, possibly including those involved in antigen uptake and concomitant antitumor immune response activation.

© 2023 International Society for Cell & Gene Therapy. Published by Elsevier Inc. This is an open access article under the CC BY license (<http://creativecommons.org/licenses/by/4.0/>)

\* Correspondence: Vincenzo Casolaro, Department of Medicine, Surgery and Dentistry 'Scuola Medica Salernitana', University of Salerno, Baronissi, Salerno, Italy

\*\* Jessica Dal Col, Department of Medicine, Surgery and Dentistry 'Scuola Medica Salernitana', University of Salerno, Baronissi, Salerno, Italy

E-mail addresses: [bmontico@cro.it](mailto:bmontico@cro.it) (B. Montico), [annnigro@unisa.it](mailto:annnigro@unisa.it) (A. Nigro), [mlamberti@exa.unrc.edu.ar](mailto:mlamberti@exa.unrc.edu.ar) (M.J. Lamberti), [dmartorelli@cro.it](mailto:dmartorelli@cro.it) (D. Martorelli),

[kmastorci@cro.it](mailto:kmastorci@cro.it) (K. Mastorci), [maria.ravo@genomix4life.com](mailto:maria.ravo@genomix4life.com) (M. Ravo), [ggiurato@unisa.it](mailto:ggiurato@unisa.it) (G. Giurato), [asteffan@cro.it](mailto:asteffan@cro.it) (A. Steffan), [Dolcetti@petermac.org](mailto:Dolcetti@petermac.org) (R. Dolcetti), [vcasolaro@unisa.it](mailto:vcasolaro@unisa.it) (V. Casolaro), [jdalcol@unisa.it](mailto:jdalcol@unisa.it) (J. Dal Col).

<sup>a</sup> These authors contributed equally to this work.

## Introduction

Cancer immunotherapies have become increasingly promising in the clinics for the ability to tune patients' immune system to find and attack tumor cells. One of the major obstacles in reaching efficient tumor cells elimination is the low immunogenicity of tumors. In this context, in recent years therapeutic approaches and anticancer agents have been re-evaluated based on their ability to promote immunogenic cell death (ICD) [1–6]. ICD is a regulated form of cell death, which enhances tumor immunogenicity by improving both antigenicity and adjuvanticity. The induction of ICD implies the exposure on cancer cell surface and/or the release of damage-associated molecular patterns (DAMPs) [7]. DAMPs are immunostimulatory ligands or secreted proteins that are evoked from the dying cancer cells; they function as adjuvants and are key elements in the induction of cellular and humoral anti-tumor immune responses. Several DAMPs have been described, including ATP, calreticulin (CRT), heat-shock proteins (HSP) 70 and 90 and high-mobility group box 1, which are now considered ICD hallmarks [8]. DAMPs can activate dendritic cells (DCs), which in turn present tumor antigens to T cells, stimulating their activation and proliferation. Therefore, ICD can promote T-cell-mediated anti-tumor immunity, which is a key mechanism for controlling cancer growth [9–13]. On these bases, the induction of ICD has become increasingly attractive as a strategy to achieve the activation of antigen-presenting cells such as DCs and the consequent elicitation of anti-tumor T-cell responses to generate long-lasting immunity [13–16]. Therefore, the main purpose of anticancer treatments should not only be limited to inducing cancer cell death but should also create an environment that efficiently permits the phagocytosis of cancer cells and the uptake of tumor-associated antigens (TAAs) [17,18]. This is imperative to permit efficient processing and presentation of TAAs by DCs together with proper co-stimulation and activation of the effector adaptive immune cells, which in turn kill malignant cells based on the specific recognition of the presented TAAs.

The molecular mechanisms and intracellular signaling involved in key events of ICD, such as DAMPs exposure and regulation of TAA presentation by tumor cells, can probably differ across the different ICD inducers used to date. Indeed, in the last decade, a large number of ICD inducers have been described having very different chemical nature and structure, as well as mode of action [16,19–21].

In the last years, we have characterized the immunological effects of the combination of 9-cis-retinoic acid (RA)/interferon (IFN)- $\alpha$ , a novel ICD inducer, in aggressive B-cell lymphoma cells. We showed that whole lysates derived from RA/IFN- $\alpha$ -treated lymphoma cells could be efficiently used as a TAAs source for the generation of antitumor DC-based vaccine [14]. Recently, we observed that RA/IFN- $\alpha$ -induced ICD was associated with enhanced expression of class I major histocompatibility complex (MHC) and reduced expression of class II MHC through the upregulation of miR-4284 and miR-212-3p [22]. We also observed that mitoxantrone and hypericin-based photodynamic therapy down-regulated MHC class II in the human melanoma A375 cell line as well [22].

Our previous study identified phospholipid scramblase 1 (PLSCR1) as one of the most important mediators of apoptosis induced by RA/IFN- $\alpha$  treatment in mantle-cell lymphoma (MCL) cells [23]. PLSCR1 is a protein with multiple functions not only in the control of apoptotic process but also in the intracellular trafficking of proteins to the plasma membrane, in the regulation of phagocytosis [24,25] and in antiviral responses [26–29]. All these characteristics prompted us to investigate whether PLSCR1 could be involved in ICD and contribute to adjuvanticity by mediating DAMPs exposure to the plasma membrane, and/or to antigenicity, by promoting TAAs recognition by cytotoxic T lymphocytes. Herein, by combining *in vitro* and *in silico* analysis, we show that: (i) the induction of PLSCR1 expression by RA/IFN- $\alpha$  occurs via STAT1 activation; (ii) ectopic expression of PLSCR1

enhances the exposure of CRT promoted during ICD induction; (iii) PLSCR1 upregulation is associated with a metagene that overrepresents genes involved in "phagocytosis recognition" and inversely correlated with "negative regulation of innate immune response" and (iv) high levels of PLSCR1 protein in tumor cell lysates used as TAAs source for DC loading elicit very efficient tumor-specific cytotoxic T lymphocytes.

## Methods

### Cell lines

MCL cell lines: Mino, Jeko-1, SP53, K562 and T2-A2 (transporter-associated with antigen-processing-deficient T2) cells stably transfected with the HLA-A\*0201 class-I molecule were used in this study. Cells were cultured in RPMI 1640 (Euroclone, Lima, Peru) supplemented with 10% fetal calf serum (FCS) (Euroclone), 100  $\mu$ g/mL streptomycin and 100 IU/mL penicillin (Sigma-Aldrich, St. Louis, MO, USA). The amphotropic-packaging cell line Phoenix (gift of Dr. G. P. Nolan, Stanford University, Stanford, CA, USA) and Granta 519 cell line were cultured in DMEM (Euroclone) supplemented with 10% FCS (Euroclone), 100  $\mu$ g/mL streptomycin, and 100 IU/mL penicillin (Sigma-Aldrich). All cell lines were maintained at 37°C in a humidified 5% CO<sub>2</sub> atmosphere. ICD was induced with human IFN- $\alpha$  (IntronA; SP Europe, Bruxelles, Belgium) and 9-cis-RA (Sigma-Aldrich) used at 1000 U/mL and 1  $\mu$ mol/L, respectively.

### Antibodies and reagents

Phospho-STAT1(Tyr701), phospho-STAT1(Ser727), STAT1, active-caspase 3 (D175), HSP70 and HSP90 antibodies were from Cell Signaling Technology (Leiden, The Netherlands); PLSCR1 antibody was from Genetex (Irvine, CA, USA), CRT antibody was from Abcam (Cambridge, UK), and  $\beta$ -tubulin and glyceraldehyde 3-phosphate dehydrogenase antibodies from Santa Cruz Biotechnology (Dallas, TX, USA). Vital nuclear dye DRAQ5, G418, and 9-cis-retinoic acid were purchased from Sigma (Saint Louis, MO, USA). IntronA was purchased from SP Europe, AG490 JAK inhibitor was purchased from Selleckchem.

### PLSCR1 ectopic expression and silencing

PLSCR1 silencing and overexpression were obtained as previously described [23]. For overexpression, the coding sequence of human PLSCR1 was obtained from TrueClone human full-length PLSCR1 cDNA by polymerase chain reaction. After *Bam*HI-*Eco*RI digestion, the PLSCR1 coding sequence product was cloned directionally in the *Bam*HI-*Eco*RI-digested pQCXIP retroviral vector. Phoenix cells were used for the transfection and supernatants from pQCXIP and pQCXIP-PLSCR1 were used for three cycles of infections. Upon infection, cells were selected with puromycin and PLSCR1 expression was verified by flow cytometry. To obtain PLSCR1 silencing, four different shRNA PLSCR1 constructs were obtained by sub-cloning the double-stranded 64-mer oligonucleotide containing the PLSCR1 target sequences (A: 5'-GGACCTCCAGGATATAGTG-3'; B: 5'-CTCTGGAGAGACCACTAAG-3'; C: 5'-AGTCTCCTCAGGAAATCTG-3') or the mismatched sequence (MIS: 5'-GGACGTCCTGGATTAGTG-3') into the pSUPER.retro.neo+GFP vector (pSUPER; OligoEngine). Infectious supernatants from pSUPER and pSUPER.retro-shPLSCR1 were used for retroviral transfection of Phoenix cells. Immunoblotting analysis of transfected Phoenix cells identified the construct shPLSCR1A as the most efficient in protein silencing, which we selected to perform all subsequent experiments. Upon infection, Mino cells were selected with G418 (1 mg/mL) and the infection efficiency was checked through the detection of GFP expression by flow cytometry (97% positive cells). Different clones of infected cells were then obtained after

seeding Mino cells in 96-well plate at an initial density of 25 cells per well in 200  $\mu$ L of medium supplemented with G418.

#### *Synthetic peptides*

A panel of 9-mer peptides was synthesized by solid-phase Fmoc chemistry (Primm srl, Milan, Italy). Purity was determined by reverse-phase high-performance liquid chromatography and verified by matrix-assisted laser desorption/ionization-time of flight analysis. Preparations of 95% pure peptides were dissolved in dimethyl sulfoxide at a concentration of 1 mg/mL and stored at  $-80^{\circ}\text{C}$  until use. We selected five HLA-A\*0201-restricted cyclin D1-derived peptides (cycD122-30: LLNDRVLRA, cycD1101-109: LLGATCMFV, cycD1195-203: FISNPPSMV, cycD1204-212: AAGSVVAAV, cycD1228-236: RLTRFLSRV).

#### *Surface detection of CRT, CD47 and HSP70*

To evaluate CRT and Hsp70 expression on membrane surface, 106 cells were re-suspended in phosphate-buffered saline (PBS) containing 0.5% bovine serum albumin (BSA), labeled with the primary antibody and incubated in ice for 30 minutes. The CRT antibody was from Abcam (Cambridge, UK), CD47, Hsp70 and 7-AADvanced Dead Cell Stain (S10349) (used to exclude dead cells from the analysis) were purchased from Miltenyi Biotec (Bergisch Gladbach, Germany).  $5 \times 10^4$  cells/sample were acquired with FACSVerse (Beckton Dickinson, Franklin Lakes, NJ, USA).

#### *Mitogen-activated protein kinase (MAPK) transcription factors assay*

To quantify the DNA-binding activity of MAPK-regulated transcription factors ATF-2, c-Jun, c-Myc, MEF2 and STAT1 we used the TransAM MAPK Family Transcription Factor assay Kit (Active Motif, Carlsbad, CA, USA), which combines a fast and user-friendly ELISA format with a sensitive and specific assay for transcription factors. Nuclear extracts of the samples were prepared according to the manufacturer's recommendations. Absorbance was read at 450 nm on a Microplate Autoreader system (Agilent BIO-TEK, Santa Clara, CA, USA).

#### *Phospho-STAT1 nuclear internalization*

In total, 106 cells per sample were fixed with 2% paraformaldehyde and permeabilized with cold methanol. After a wash with PBS containing 0.5% BSA, cells were incubated with an antibody against phospho-STAT1(Y701) (1:30) at  $4^{\circ}\text{C}$  overnight. After two washes with PBS/0.5% BSA, cells were incubated for 30 minutes in ice with PE-anti-rabbit secondary antibody. Finally, DRAQ5 nuclear dye was added, then cells were acquired with the Amnis ImageStreamX instrument (Luminex Co., Austin, TX, USA) using the INSPIRE software. Only viable cells were selected based on morphologic features, and only phospho-STAT1 positive cells were analyzed. The similarity score (SS) [30] between phospho-STAT1 and DRAQ5 staining was calculated for each sample. To define the range of variability of the SS, the lower and the upper limits were calculated. Specifically, the negative control sample was labeled with DRAQ5 and an antibody against tubulin (cytoplasmic marker) and the score value was  $-1.316 \pm 0.5538$  (SS  $\pm$  standard deviation). The positive control sample was labeled with DRAQ5 and an antibody against PARP (nuclear marker) and the score value was  $2.426 \pm 0.4956$  (SS  $\pm$  standard deviation).

#### *Tumor cell lysates preparation and western blot analyses*

Total protein extracts were obtained as previously described [31]. Total lysates were quantified with Bio-Rad Protein Assay. To obtain membrane and cytoplasmic fractions, Pierce Cell Surface Protein

Isolation Kit was used. Tumor cell lysates (TCLs) for DC pulsing were obtained re-suspending  $5 \times 10^6$  cells in 100  $\mu$ L of sterile PBS and by three rapid freeze-thaw cycles, then lysates were centrifuged at 13 000 rpm (15 min,  $4^{\circ}\text{C}$ ) and the recovered supernatants were quantified and diluted in PBS to 1 mg/mL and used for immunoblotting analysis and DC pulsing.

Proteins were separated by sodium dodecyl sulfate-polyacrylamide gel electrophoresis and transferred onto nitrocellulose membranes. After blocking with 5% milk for at least 1 h, the membrane was stained with primary antibodies at  $4^{\circ}\text{C}$  overnight then labeled with horseradish peroxidase-conjugated secondary antibodies. Immunoblotting was performed using the enhanced chemiluminescence detection system (Clarity, 1705061; Bio-Rad, Hercules, CA, USA). Detailed description of the antibodies used for WB is reported in [supplementary Table 1](#).

#### *IFN-DC generation*

IFN-DCs were obtained by following the protocol published in [32]. To summarize, CD14<sup>+</sup> monocytes were isolated with anti-CD14-coated micro beads (130-050-201; Miltenyi Biotec, Bergisch Gladbach, Germany) from human peripheral blood mononuclear cells collected from healthy donors' buffy coats, following the manufacturer's instructions. Monocytes were then cultured 3 days in 6-well plates ( $5 \times 10^6$  cells/well) with CellGenix GMP DC medium (CellGenix GmbH, Freiberg, Germany) with the addition of 10 000 UI/mL IFN- $\alpha$  and 50 ng/mL recombinant human GM-CSF (PromoKine, Heidelberg, Baden-Württemberg, Germany) to achieve DC maturation. After maturation, DCs were then pulsed O.N. with different types of TCLs (protocol described above) depending on the specific assay.

#### *In vitro phagocytosis assay*

Mino, Mino-empty and Mino-PLSCR1 cells were labeled with Fast DiA cell-labeling solution according to the protocol (D7758; Molecular Probes, Eugene, OR, USA) then treated or not with RA/IFN $\alpha$ . TCLs (obtained as described previously) or cells were then co-cultured with IFN-DCs at a ratio of 1:3 for 4 h. At the end of the incubation, cells were harvested, washed and stained with CD11 c-PC5 antibody. Phagocytosis was assessed by multi-spectral imaging flow cytometry.

#### *Cytotoxic T lymphocyte generation and cytotoxicity assay*

Cytotoxic T lymphocytes were generated by co-culturing TCL-pulsed IFN-DC with autologous peripheral blood lymphocytes and were re-stimulated weekly four times. To assess tumor-specific Cytotoxic T lymphocytes activation, standard calcein-AM release assays were performed. Mino plain (not infected), Mino-empty (infected with empty vector pQCXIP virus), Mino-PLSCR1 (infected with pQCXIP-PLSCR1 virus), Mino-pSuper or Mino-shPLSCR1 (clones 5 and 6) were used as target cells depending on the specific assay. Target cells were re-suspended in Hank's Balanced Salt Solution (Sigma-Aldrich) added with 5% FCS and labeled 90 min at  $37^{\circ}\text{C}$  and 5% CO<sub>2</sub> with calcein-AM (Invitrogen, Carlsbad, CA, USA). T2-A2 cells were loaded for 2 h with HLA-A\*0201 restricted peptides derived from cyclin D1. Standard calcein-AM detection was performed. To summarize, after three washes, target cells were seeded in V-bottom 96-wells plates, and effector CTLs were added at a 10:1 effector/target ratio. The intensity of released calcein-AM was assessed after a 4-h incubation at  $37^{\circ}\text{C}$  and 5% CO<sub>2</sub> by using a SpectraFluorPlus fluorimeter (Tecan).

#### *RNA purification, sequencing and data analysis*

Total RNA was extracted as described previously [33]. Indexed libraries were prepared from 1  $\mu$ g/ea. purified RNA with TruSeq

Stranded Total RNA Sample Prep Kit (Illumina Inc., San Diego, CA, USA) according to the manufacturer's instructions. Libraries were sequenced (paired-end,  $2 \times 100$  cycles) at a concentration of 8 pmol/L per lane on a HiSeq2500 platform (Illumina Inc.). The raw sequence files generated (fastq files) underwent quality control analysis using FastQC (<http://www.bioinformatics.babraham.ac.uk/projects/fastqc/>) and the quality checked reads were then aligned to the human genome (hg19 assembly) using TopHat version 2.0.10 [34], with standard parameters. A given mRNA was considered expressed when detected by  $\geq 10$  reads. Differentially expressed mRNAs were identified using DESeq version 1.14.0 [35]. First, gene annotation was obtained for all known genes in the human genome, as provided by Ensemble (GRCh37). Using the reads mapped to the genome, we calculated the number of reads mapping to each transcript with HTSeq-count [36]. These raw read counts were then used as input to DESeq for calculation of normalized signals for each transcript in the samples, and differential expression was reported as Fold Change along with associated adjusted  $P$ -values (computed according to Benjamini-Hochberg).

### Bioinformatic analysis

For *in silico* analysis of RNAseq data comparing untransfected (plain) with PLSCR1-overexpressing Mino, significant differentially expressed genes (DEGs) were defined with a threshold for the  $\text{Log}_2$ (-fold change) to 0.6 (fold change = 1.5) and  $-\text{Log}_{10}(P \text{ value})$  to 1.3 ( $P \text{ value} < 0.05$ ). The volcano plots were generated with VolcanoR [37], and significant hits are depicted in yellow for upregulated and in blue for downregulated genes. The annotated dots are the ten data points that have the largest (Manhattan) distance from the origin and are above the thresholds indicated by the dashed line. GSEA was used to conduct enrichment analysis of gene expression data [38]. To select gene set databases, literature search was done to identify immunogenicity-associated parameters within Gene Ontology Biological Process [39–41]. To identify the gene sets enriched in the samples analyzed, normalized enrichment score (NES) and the FDR

(false discovery rate) values were used to classify the pathways (gene sets) as activated (NES  $> 0$ , FDR  $< 25\%$ ), inhibited (NES  $< 0$ , FDR  $< 25\%$ ) or neither (FDR  $> 25\%$ ).

For *in silico* analysis of RNAseq data comparing “empty-vector (empty) versus PLSCR1-overexpressing Mino” with “RA/IFN $\alpha$  versus Control” (from E-MTAB-11799), significant DEGs were defined with a threshold for fold change = 1.3 and  $P \text{ value} < 0.05$ . Those parameters were previously used with the latter database [22]. Analysis of DEGs lists through Venn diagrams was carried out using the InteractiVenn online tool [42]. Gene Ontology and Kyoto Encyclopedia of Genes and Genomes–based-enrichment analysis was performed for the common upregulated DEGs, using the g:GOST tool in gProfiler (<https://biit.cs.ut.ee/gprofiler/>) [42]. The Ggplot2 package in R was used for bar plotting [43]. The RNAseq table with the raw counts is available in figshare (<https://doi.org/10.6084/m9.figshare.22283860>).

### Statistical analysis

Data from flow cytometry and cytotoxicity assays were analyzed using Student's paired  $t$ -test. A  $P \text{ value} < 0.05$  was considered statistically significant (\* $P < 0.05$ , \*\* $P < 0.01$ ). Statistical analysis was performed using GraphPad Prism 5 (GraphPad Software, Inc., La Jolla, CA, USA).

## Results

### RA/IFN- $\alpha$ combination induces PLSCR1 expression via STAT1 activation in MCL cells

TCLs were obtained from SP53 and Mino MCL cell lines untreated or treated with RA/IFN- $\alpha$  for 5 days, and subsequently they were used to load IFN-conditioned DCs [44,45] as schematically shown in Figure 1A. TCL-pulsed DCs, generated from HLA-matched healthy donors, were exploited for the *in vitro* generation of tumor-specific cytotoxic T lymphocytes (see the Methods section). DCs loaded with RA/IFN- $\alpha$ -treated TCLs were significantly more efficient in eliciting

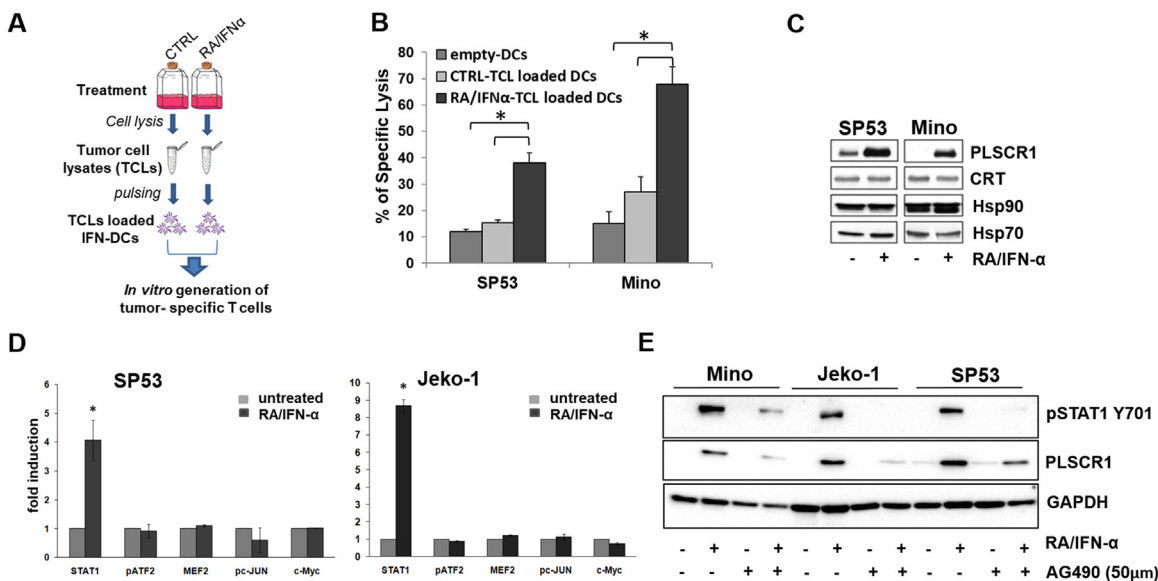


**Figure 1.** PLSCR1 protein expression is upregulated during RA/IFN- $\alpha$ -induced ICD via STAT1 activation. (A) Schematic representation of the protocol for the generation of tumor-specific T lymphocytes using whole TCLs as TAA source. (B) HLA-A\*0201-restricted healthy donor-derived lymphoma-specific cytotoxic T-cell cultures were evaluated for their killing activity against MCL cell lines by standard calcein-AM release assay. (\* $P < 0.05$ , Student's  $t$ -test). The graph represents the mean of three independent experiments with cells from different healthy donors. All tests were performed in triplicate at effector/target ratio of 20:1. (C) Immunoblotting analysis of whole protein extracts obtained from SP53 and Mino cells treated with dimethyl sulfoxide or RA/IFN- $\alpha$  combination for 4 h. Specific antibodies against the indicated protein were used. (D) SP53 and Jeko-1 cells were treated or not with RA/IFN- $\alpha$  for 4 h. A total 15  $\mu\text{g}$  of nuclear protein extracts was analyzed for the DNA-binding activity of the indicated transcription factors using TransAM MAPK family transcription factors assay. Assay was performed in triplicate. (\* $P < 0.05$ , Student's  $t$ -test). (E) Mino, SP53 and Jeko-1 cell lines were treated for 1 h with AG490 inhibitor (50  $\mu\text{mol/L}$ ) and successively exposed to RA/IFN- $\alpha$  treatment for 24 h. STAT1 phosphorylation and PLSCR1 expression were assessed by immunoblotting. Glyceraldehyde 3-phosphate dehydrogenase (GAPDH) was assessed as loading control.

lymphoma-specific T-cell-mediated cytotoxic activity as compared with DCs loaded with untreated TCLs or unpulsed DCs (empty-DCs) (Figure 1B and supplementary Figure 1A). Of note, cytotoxic T-cell cultures generated with autologous DCs, loaded with SP53- and Mino-TCLs, were able to recognize and kill another MCL cell line (Granta 519), whereas their specific lytic activity was impaired by the lack of MHC class I expression against K562 cell line (supplementary Figure 1B). RA/IFN- $\alpha$ -promoted apoptosis was associated to the induction of PLSCR1 protein expression in Mino, SP53 and Jeko-1 cell lines (supplementary Figure 2A). In our previous study [23], we demonstrated that PLSCR1 has a pro-apoptotic activity, which is confirmed herein as we show that PLSCR1 knock-down by a short hairpin RNA expression vector (shPLSCR1) decreased RA/IFN- $\alpha$ -induced PARP-1 cleavage (supplementary Figure 2A,B). Immunoblotting analysis of whole protein extracted after 48 h of RA/IFN- $\alpha$  treatment revealed that besides PLSCR1, none of the established ICD hallmarks, such as CRT, HSP70 and 90, were differentially enriched in RA/IFN- $\alpha$ -treated lymphoma cells compared to the untreated ones (Figure 1C).

PLSCR1 is an IFN-induced gene whose expression can be regulated by several transcription factors including STAT1, c-Myc, c-Fos, Snail and others [25,46–48]. Using a NoShift transcription factor assay (Active Motif, Carlsbad, CA, USA) for different proteins, we

demonstrated that RA/IFN- $\alpha$  treatment specifically increased STAT1 activity (Figure 1D) in both SP53 and Jeko-1 cell lines, whereas it did not affect other transcription factors such as ATF2, c-Myc, MEF-2 and c-Jun. Immunoblotting analysis confirmed STAT1 phosphorylation/activation at tyrosine 701 (Y701) following RA/IFN- $\alpha$  treatment in Mino, SP53 and Jeko-1 cells (Figure 1E). Pre-treatment of MCL cells with the JAK inhibitor AG490 (50  $\mu$ mol/L) for 1 h impaired RA/IFN-induced STAT1 phosphorylation/activation and the consequent up-regulation of PLSCR1 expression (Figure 1E).

Moreover, a time course assay showed that the treatment rapidly increased STAT1 phosphorylation at both Y701 and serine(S)727, which was detectable just 15 minutes after treatment (Figure 2A). The analysis of phospho-STAT1 nuclear translocation by multi-spectral imaging flow cytometry confirmed the presence of activated STAT1 into the nucleus after RA/IFN- $\alpha$  stimulation (Figure 2B). The results showed that the percentage of cells showing nuclear phospho-STAT1 Y701 expression was significantly increased in both cell lines after 15 min of treatment, remained quite constant for 2 h, then started to decrease from 74% to 23% in SP53, and from 78% to 65% in Jeko-1 cells. Altogether, these results indicated that RA/IFN- $\alpha$  treatment induced STAT1 phosphorylation and increased its activity, suggesting a role for this transcription factor in mediating RA/IFN- $\alpha$ -dependent PLSCR1 up-regulation.

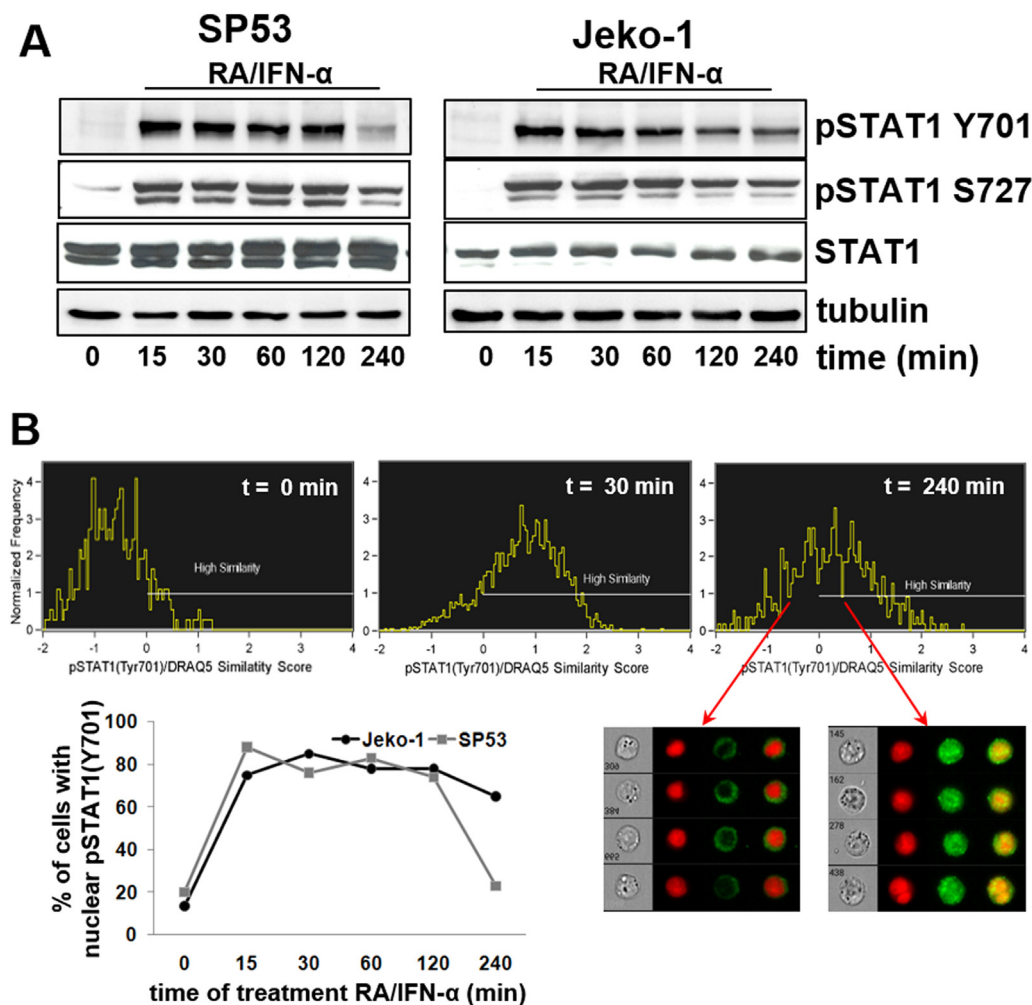


**Figure 2.** RA/IFN- $\alpha$  treatment promotes STAT1 nuclear internalization. (A) SP53 and Jeko-1 cells were treated with RA/IFN- $\alpha$  combination and the phosphorylation of STAT1 on Y701 and S727 sites was evaluated at the indicated time points. Tubulin was used as loading control. (B) RA/IFN- $\alpha$ -treated MCL cells were harvested at the indicated time points. In total,  $2 \times 10^4$  cells were acquired with ImageStream X and phospho-STAT1 nuclear localization was calculated as SS between phospho-STAT1 and DRAQ5 intensities. All events showing a positive SS were considered cells with nuclear localization of phospho-STAT1. Data are representative of one of two independent experiments.

### Ectopic expression of PLSCR1 boosts RA/IFN- $\alpha$ -induced surface exposure of CRT

Our previous data demonstrated that PLSCR1 is involved in mediating the pro-apoptotic activity exerted by RA/IFN- $\alpha$  treatment [23], following which we showed that immunogenic RA/IFN- $\alpha$ -induced dying/dead cells had anticancer vaccine effects when implanted in syngeneic mice [14]. These findings allowed us to define the RA/IFN- $\alpha$  combination as a novel ICD inducer. Based on these considerations, herein we investigated the potential involvement of PLSCR1 in ICD promoted by RA/IFN- $\alpha$  in MCL cells. Taking into account that PLSCR1 is a transmembrane protein involved in the subcellular trafficking of several proteins and receptors [49–51], we evaluated first its subcellular localization following RA/IFN- $\alpha$  treatment, and second, its involvement in the cell surface exposure of such ICD markers as CRT and Hsp70. Immunoblot analysis of intracellular and membrane protein fractions revealed the presence of PLSCR1 in both compartments of RA/IFN- $\alpha$ -treated Mino cells together with CRT and HSP70 (Figure 3A). Thus, using a previously established cell line expressing ectopic PLSCR1 (Mino-PLSCR1+), shown in Figure 3B, we investigated by flow cytometry the surface expression of CRT (ecto-CRT) and HSP70. In addition, given that ecto-CRT exerts a distinctive “eat me” function that counterbalances “don’t eat me” signals from surface CD47 [52,53], we extended our analysis to CD47, which is not considered a conventional ICD marker per se. Whereas the ectopic expression of PLSCR1 itself was not sufficient to induce ecto-CRT expression, it significantly enhanced its levels following RA/IFN- $\alpha$  treatment (Figure 3B). Conversely, PLSCR1 overexpression did not alter the effects of the treatment on CD47 and HSP70 (Figure 3C,D). Confirming the pro-phagocytic function of ecto-CRT, Mino PLSCR1+ cells treated with RA/IFN- $\alpha$  were more efficiently engulfed *in vitro* by IFN-conditioned DCs compared to Mino cells transfected with the empty vector (Figure 3E,F). In parallel with CRT regulation, the ectopic expression of PLSCR1 alone was not sufficient to improve tumor cell phagocytosis by DCs. These data support the hypothesis that the presence of PLSCR1 can enhance CRT exposure induced by ICD revealing its putative role as an adjuvant protein increasing ICD-associated immunogenicity.

### PLSCR1 overexpression modulates transcriptional program of MCL cells

We aimed to identify genes whose expression was selectively modulated by high levels of PLSCR1. Transcriptomic analysis of Mino cells showed that overexpression of PLSCR1 led to a transcriptional program characterized by up-regulated expression of 735 genes and suppression of 882 genes (Figure 4A). In line with a potential implication of PLSCR1 in modulating immunogenic features of ICD, gene set enrichment analysis revealed that genes associated with “phagocytosis recognition” were up-regulated in PLSCR1+ lymphoma cells, whereas genes associated to “negative regulation of innate immune response” were down-regulated (Figure 4B). Moreover, to assess if PLSCR1 could mediate some transcriptional effects of RA/IFN- $\alpha$ -induced ICD in Mino cells [22] we performed a comparative RNAseq data analysis. This comparison enabled us to identify 65 up-regulated and 51 down-regulated genes shared between PLSCR1 overexpressing and RA/IFN- $\alpha$ -treated Mino cells (Figure 4C). Intriguingly, among the down-regulated genes we identified CD276 and CD84, both contributing to cancer cell immune evasion given their immunosuppressive functions in the tumor microenvironment [54,55]. On the other hand, gene ontology analysis of the combined data sets revealed that genes up-regulated by both ICD and PLSCR1 were related to the inflammatory response and enriched for “NOD-like receptor signaling,” while the modulation of a lipid-associated metagene supported their involvement in phagocytosis regulation (Figure 4D).

### TCLs obtained from PLSCR1 overexpressing tumor cells are a suitable source of TAA for DC-based vaccine

As shown in Figure 1A,B and in our previous work [14], RA/IFN- $\alpha$ -derived TCLs are exploitable as a TAA source for loading DC for vaccination purposes. Consistently, RA/IFN- $\alpha$ -derived TCLs shared with apoptotic cells the expression of relevant ICD markers [14]. In addition, RA/IFN- $\alpha$  TCLs contained detectable levels of PLSCR1, as shown in Figure 5A. Therefore, in order to investigate the role of PLSCR1 in mediating the ability of RA/IFN- $\alpha$  TCLs-loaded DCs to activate MCL-specific cytotoxic T lymphocytes, we obtained TCLs from Mino cells transfected with empty or PLSCR1+ expression vectors (Figure 5A) and used them to pulse DCs. Hence, cytotoxic T lymphocytes were generated by co-culturing unpulsed and TCL-pulsed DC from HLA-matched donors, and T-cell activation was measured by analyzing the extent of specific lytic activity. IFN-conditioned DCs were pulsed with different types of TCLs derived from untreated (CTRL), RA/IFN- $\alpha$ -treated, empty-vector and PLSCR1+ Mino cells and subsequently used to generate cytotoxic T lymphocytes as summarized in Figure 5B. Notably, PLSCR1+ TCL-pulsed DCs, similarly to RA/IFN- $\alpha$  TCL-pulsed DCs, were able to induce T-cell populations with significantly greater and more efficient killing activity compared with CTRL-TCL-pulsed DCs and Empty-TCL-pulsed DCs (Figure 5C and supplementary Figure 3). These results indicated that PLSCR1 boosts the immunogenic potential of TCLs resulting in a more efficient activation of DCs. When PLSCR1+ Mino cells were used as target cells, they were recognized and killed with comparable efficiency to Mino plain/untransfected cells (Figure 5C). Conversely, Mino cells transfected with empty vector were poorly recognized and killed by even the most efficiently primed cytotoxic T lymphocytes (Figure 5C).

To confirm the contribution of PLSCR1 to the enhanced immunogenicity of RA/IFN- $\alpha$ -derived TCLs, we conducted parallel experiments in a Mino cell line in which PLSCR1 was knocked-down (shPLSCR1), owing to which it was less responsive to induction by RA/IFN- $\alpha$  treatment [23] (supplementary Figure 2A,B). In these experiments, we generated cytotoxic T lymphocytes by co-culturing DCs loaded with TCLs obtained from untransfected (plain) Mino cells, tumor cells transfected with empty vector (pSuper) and two independent clones (cl.5 and cl.6) of tumor cells transfected with short-hairpin RNA expressing vector (shPLSCR1) treated or not with RA/IFN- $\alpha$ . Indeed, PLSCR1 silencing in shPLSCR1-RA/IFN- $\alpha$ -treated TCLs impaired T-cell-mediated cytotoxic responses against several HLA-A\*0201-restricted cyclin D1-derived epitopes, compared with T lymphocytes stimulated with RA/IFN- $\alpha$  treated pSuper or plain-TCLs loaded DCs (Figure 6). These findings indicated that the induction of PLSCR1 expression by RA/IFN- $\alpha$  during ICD exerts a positive influence on the immunogenicity of TCLs obtained from dying/dead cells.

## Discussion

One of the major challenges of cancer immunotherapy is counteracting the multiple strategies developed by tumor cells to avoid their detection and elimination by the immune system. Cancer cells may downregulate tumor antigen presentation, exploit physiological immune checkpoint mechanisms or favor the development of an immune suppressive tumor microenvironment. Moreover, tumor cell plasticity leads to the development of several mechanisms of immune evasion that can determine the failure of such immunotherapeutic approaches, such as the administration of immune checkpoint inhibitors [56,57]. Developing new therapeutic strategies that can support and boost currently approved immune checkpoint inhibitor therapy in oncology is an active area of research.

Inducing ICD can be a strategy for improving anticancer immune responses. Nevertheless, there are several difficulties to achieve successful ICD in patients, including the resistance to ICD-inducing treatments, a limited immune system activation, the tumor

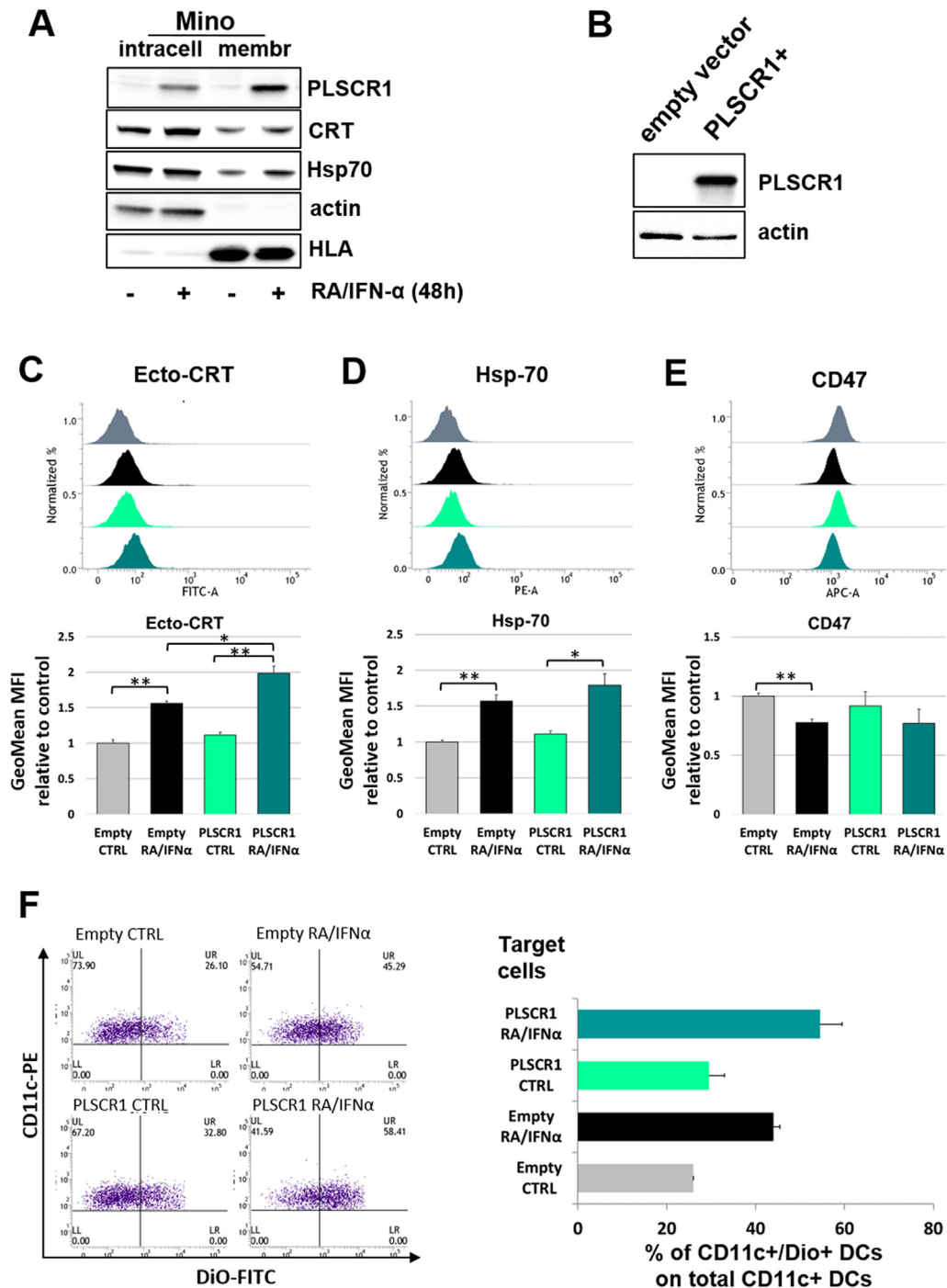


**Figure 3.** PLSCR1 enhances RA/IFN- $\alpha$ -promoted CRT exposure on cell membrane and consequent tumor cell phagocytosis by DCs. (A) Mino cells were treated for 48 h with RA/IFN- $\alpha$ . Intracellular and plasma membrane fractions were separated for immunoblotting. Actin and HLA were analyzed as loading controls for cytoplasmic and plasma membrane fractions, respectively. (B) Ectopic expression of PLSCR1 was shown by immunoblotting of protein extracts obtained from Mino cells transfected with pQCXIP (empty vector) or pQCXIP-PLSCR1 (Mino-PLSCR1+). Actin was analyzed as loading control. (C–E) Transfected Mino cells (empty and PLSCR1+) were treated with RA/IFN- $\alpha$  for 48 h and the expression of ecto-CRT (C), Hsp70 (D) and CD47 (E) on cell surface was analyzed by flow cytometry. Representative histogram of fluorescence (upper panel) and the mean of three independent experiments (lower panel) are shown (\* $P < 0.05$ , \*\* $P < 0.01$  Student's  $t$ -test). (F) Phagocytosis assay. Representative flow cytometric analyses and mean  $\pm$  SEM (N = 2 independent experiments) of phagocytic activity of monocyte-derived dendritic cells (see Methods) against Mino cells transfected with pQCXIP (Empty) or with pQCXIP-PLSCR1 (PLSCR1+) untreated or treated with RA/IFN- $\alpha$ . Cancer cells exposed to the treatment for 48 h were labeled with DiO tracer then co-cultured with DCs for 2 hours at a 1:3 ratio. Histograms represent the percentages of positive cells for both CD11c and DiO tracer relative to total DCs.

heterogeneity, the timing and the dosing, among others [58]. A better understanding of the mechanisms underlying ICD and of the molecules involved in this process could help identify novel factors with immune-modulating effects and promote the development of new immunotherapeutic approaches.

In line with these considerations, the present study investigated the regulation of PLSCR1 expression by the RA/IFN- $\alpha$  combination and PLSCR1 contribution to RA/IFN- $\alpha$ -induced ICD. Our previous work, through transcriptome profiling, had identified PLSCR1 as one of the most upregulated pro-apoptotic proteins upon RA/IFN- $\alpha$

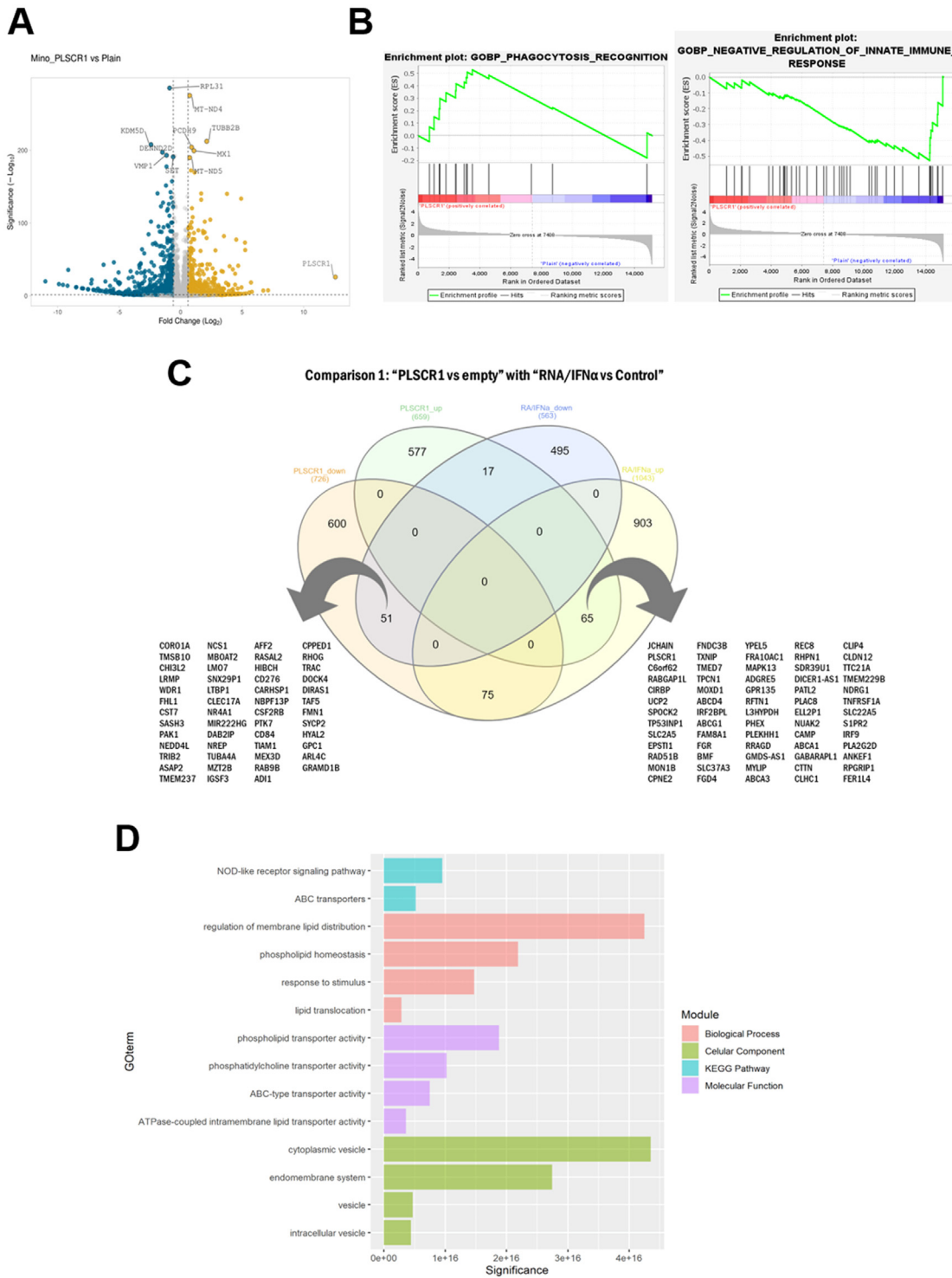


**Figure 4.** Ectopic expression of PLSCR1 modifies the transcriptional profile of lymphoma cells associated to immune response and recapitulates RA/IFN- $\alpha$  signaling. (A) Volcano plot of differentially expressed genes (DEGs) between untransfected (plain) and PLSCR1-overexpressing Mino (Mino\_PLSCR1). Significant hits are depicted in yellow for up-regulated and in blue for down-regulated genes. (B) Gene sets over- or under-represented in these samples following gene set enrichment analysis. (C) Venn diagrams showing significant DEGs interaction between RNAseq data comparing "PLSCR1-overexpressing versus empty-vector (empty)" with "RA/IFN- $\alpha$  versus Control" Mino (from E-MTAB-11799). (D) Gene Ontology and Kyoto Encyclopedia of Genes and Genomes–based-enrichment analysis performed for the shared up-regulated DEGs. (For interpretation of the references to colour in this figure legend, the reader is referred to the web version of this article.)

treatment in MCL cells [23]. Moreover, we reported that RA/IFN- $\alpha$  combination was able to control both PLSCR1 mRNA transcription and protein degradation [23]. Type I IFN pathway activation is currently known as a feature of ICD and postulated as a novel inducible source of DAMPs [21,59–61]. Nevertheless, the involvement in ICD of specific IFN-inducible factors has not been thoroughly investigated.

This study shows that, in the context of ICD induction in MCL cells, RA/IFN- $\alpha$  treatment enhanced PLSCR1 expression by activating STAT1. Earlier evidence demonstrated that PLSCR1 expression is strongly induced in response to type I IFNs [46,62,63]. In particular, STAT1 is required for PLSCR1 gene transcription in response to IFN- $\alpha$  stimulation [46] and, in turn, PLSCR1-STAT3 heterodimer formation

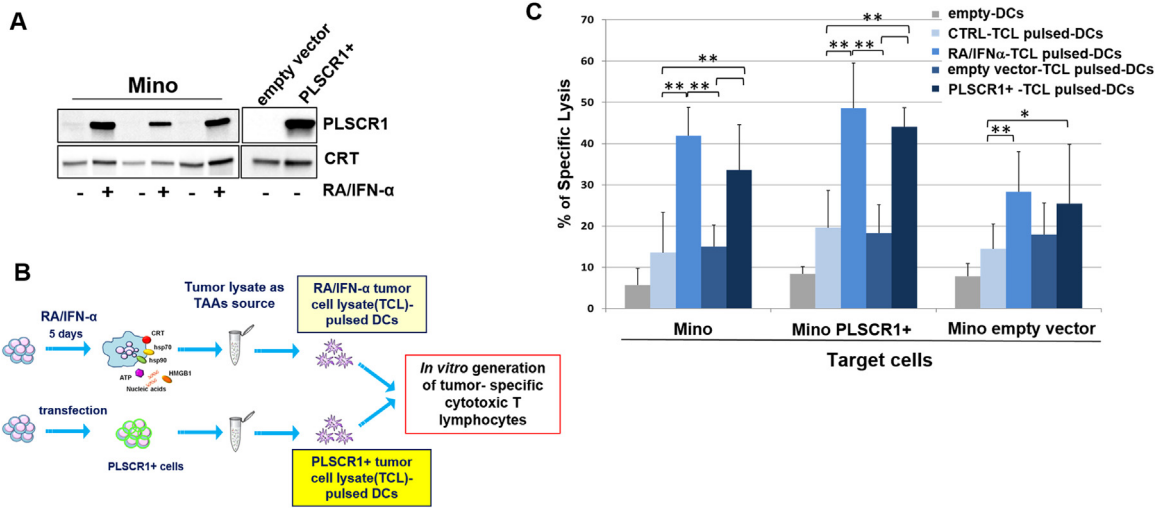


**Figure 5.** DCs loaded with TCLs obtained from Mino cells expressing ectopic PLSCR1 elicit anti-tumor T-cell mediated responses with comparable efficacy to RA/IFN- $\alpha$ -TCLs loaded DCs. (A) Immunoblotting analysis of TCLs obtained from Mino cells untreated or treated with RA/IFN- $\alpha$  for 5 days (in triplicates) or from Mino transfected with pQCXIP (empty vector) or pQCXIP-PLSCR1 (Mino-PLSCR1+). (B) Schematic representation of the protocol for generation of tumor specific T lymphocytes using TCLs in (A) as TAAs source. (C) HLA-A\*0201-restricted healthy donor-derived cytotoxic T lymphocytes were evaluated for their killing activity against Mino, Mino PLSCR1+ and Mino empty vector cell lines by standard calcein-AM release assay ( $^*P < 0.05$ ,  $^{**}P < 0.01$ ; Student's *t*-test). The graph represents a mean of five independent experiments with cells from different healthy donors. All tests were performed in triplicate at effector/target ratio of 10:1.

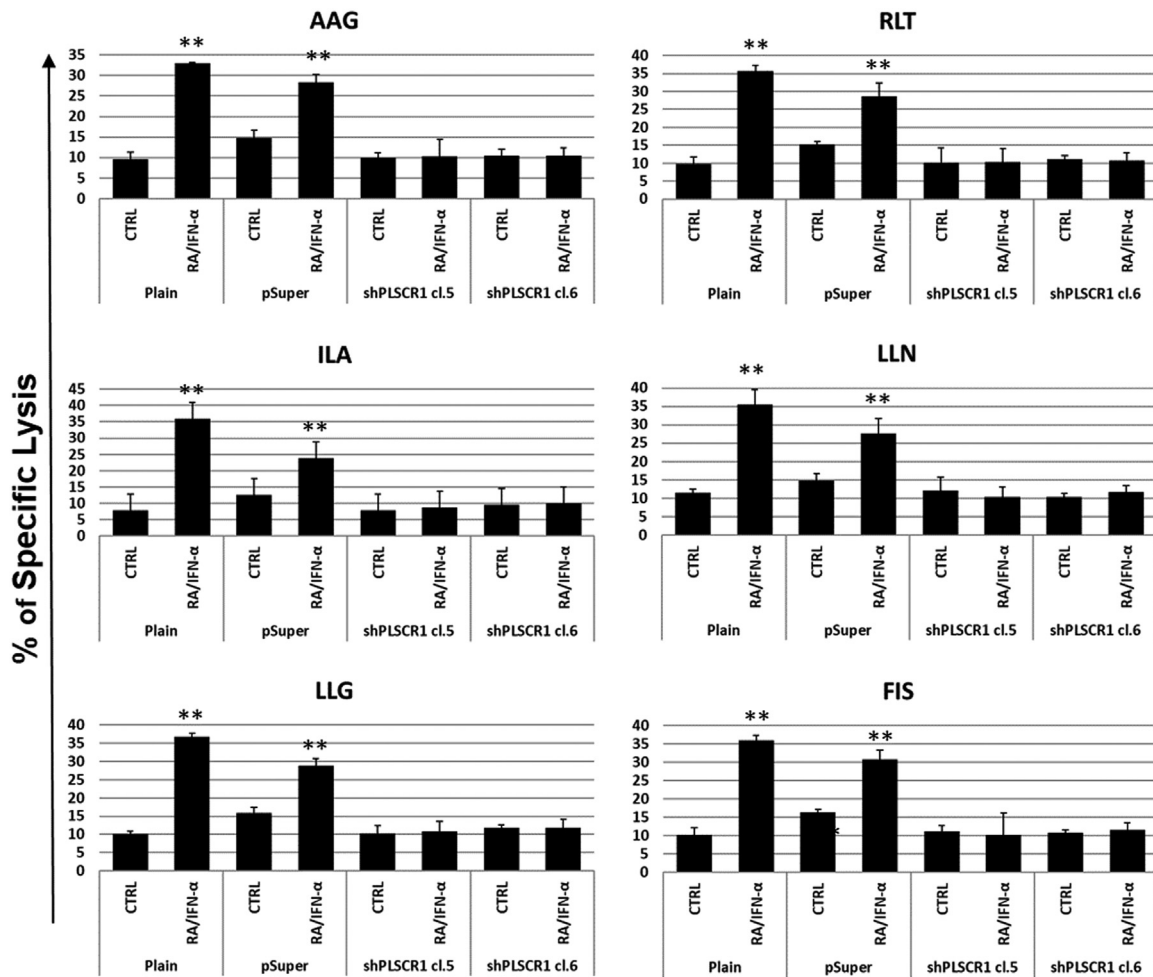


**Figure 6.** shPLSCR-infected Mino TCLs cannot prime cyclin D1-specific cytotoxic T lymphocytes responses. HLA-A\*0201 polyclonal cytotoxic T lymphocytes were generated using DCs loaded either with parental (Plain) or infected (pSuper, shPLSCR cl.5 and shPLSCR cl.6) Mino lysates after RA/IFN- $\alpha$  treatment. Untreated lysates were used as negative controls (CTRL). Cytotoxic activity against cyclin D1 peptide-loaded T2-A2 cells was characterized by standard calcein-AM release assay. All tests were performed in triplicate at effector/target ratio of 40:1. HLA-A\*0201-restricted cyclin D1-derived peptides AAG (cycD1204-212: AAGSVVAAV), RLТ (cycD1228-236: RLTRFLSRV), LLN (cycD122-30: LLNDRVLRA), LLG (cycD1101-109: LLGATCMFV), FIS (cycD1195-203: FISNPPSMV).

into the nucleus can induce transcriptional activation of STAT1, thus amplifying the effects of IFN [46,64]. However, the relationship between PLSCR1 and STAT proteins may vary depending on the context of the cellular response [64]. Further studies are needed to fully elucidate the mechanisms underlying PLSCR1 regulation and its interactions with other signaling pathways.

Although several studies showed that PLSCR1 has been implicated in both cell death [23,65–67] and immune responses [68–71], its potential role in ICD has not been yet investigated. One of the most documented functions of PLSCR1 is the exposure of phosphatidylserine on the surface of dying cells [72], an important signal for the recognition and clearance of apoptotic cells by phagocytes [24,73]. During ICD, the exposure of CRT on the surface of dying cells acts as an “eat me” signal as well, promoting their phagocytosis by antigen-presenting cells, such as DCs. Differently from phosphatidylserine, which is flipped from the inner to the outer leaflet of the plasma membrane, CRT is translocated from the endoplasmic reticulum to the cell surface through a highly regulated process that involves the protein Erp57 [74]. Herein, we document that ectopic expression of PLSCR1 increased the surface expression of CRT in response to RA/IFN- $\alpha$  treatment and concomitantly enhanced the engulfment of dying cells by DCs. Nevertheless, PLSCR1 overexpression alone is not sufficient to promote CRT surface expression or DCs-mediated phagocytosis. This suggests that PLSCR1 could play a role in modulating the translocation of CRT specifically during ICD induced by RA/IFN- $\alpha$  or possibly other agents. In other cellular models, PLSCR1 regulates the intracellular trafficking of receptors and membrane proteins, such as the epidermal growth factor receptor, the Toll-like receptor-9 and BACE  $\beta$ -secretase [49,51,75] via direct interaction. Therefore, PLSCR1 may affect CRT translocation by interacting with other proteins, like Erp57. Further studies are needed to elucidate the mechanism by which PLSCR1 modulates CRT surface expression (Figure 7).

Transcriptome profiling provided insights into the specific genes and pathways that are activated in response to PLSCR1 overexpression in MCL cells and possibly account for its immunogenic properties. As expected, we found that PLSCR1 induced the upregulation of genes involved in “phagocytosis recognition.” In addition, transcriptome profiling revealed potential downstream targets of PLSCR1 signaling associated to “negative regulation of innate immune response.” Interestingly, the integrative analysis with RNA-seq data from MCL cells undergoing ICD induced by RA/IFN- $\alpha$  [22] uncovered the NOD-like receptor (NLRs) pathway as a common enriched signature. When DAMPs are released from cells undergoing ICD, they can be recognized by NLRs, which in turn activate downstream signaling pathways that lead to the activation of the inflammasome. The inflammasome triggers the production of pro-inflammatory cytokines such as IL-1 $\beta$ , which in turn can stimulate the immune response [76,77]. However, more studies will be needed to fully understand the mechanisms underlying the activation of NLR signaling mediated by PLSCR1 and its putative association with ICD. Moreover, the enrichment of up-regulated genes for intracellular/cytoplasmic vesicles and endomembrane system as cellular components suggested a possible contribution of PLSCR1 to the intracellular trafficking of molecules or eventually of processed TAAs.

*Ex vivo* ICD, which refers to the induction of ICD in cancer cells in a laboratory setting, can be used to generate immunogenic TCLs exploitable as source of TAAs in DC-based vaccine development [13]. DCs vaccines have yielded promising results in preclinical studies and some clinical trials for the treatment of various types of cancer, including melanoma, follicular lymphoma, prostate cancer and glioblastoma, among others [78–84]. In line with these studies, the surface shuttling of CRT has been demonstrated to play a critical role in ICD not only during the cell death process but also when dying/dead tumor cells have been used for *ex vivo* DC loading [14,79,85].

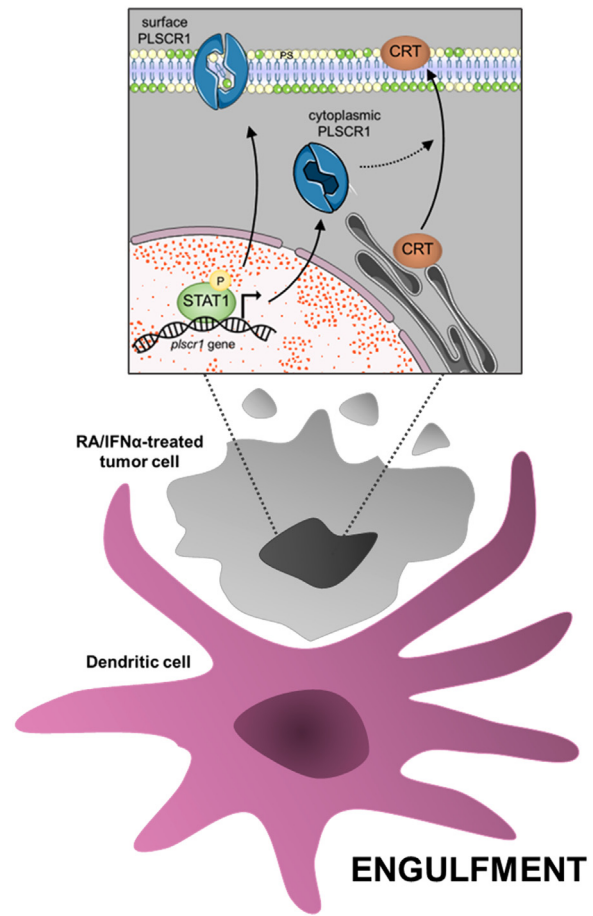


**Figure 7.** Phagocytosis enhancement in RA/IFN- $\alpha$ -treated tumor cells upregulated by both ICD-induced and ectopic PLSCR1 expression. In the context of ICD induction in tumor cells, treatment with RA/IFN- $\alpha$  activates STAT1, resulting in enhanced expression of PLSCR1 both in the cytoplasm and on the cell surface. Surface-expressed PLSCR1 plays a critical role in facilitating the exposure of phosphatidylserine on the surface of dying cells, serving as a vital “eat me” signal for phagocyte recognition and clearance of apoptotic cells. Notably, during ICD mediated by RA/IFN- $\alpha$ , ectopic expression of PLSCR1 leads to increased translocation of CRT from the endoplasmic reticulum to the cell membrane. This phenomenon concomitantly augments the engulfment of dying cells by DCs, further enhancing the immunogenicity of the process.

Similarly, independent studies described the impact of other specific ICD-associated DAMPs, such as HSP70, on immature and mature DCs [18,86]. Herein, we have demonstrated that PLSCR1 overexpression, obtained by genetic approach or through transcriptional upregulation following ICD induction, positively influences the immunogenicity of TCLs. In particular, TCLs obtained from cells overexpressing PLSCR1 improve the ability of DCs to stimulate tumor-specific T-cell cytotoxicity, presumably by improving the processing and/or presentation of TAA/epitopes. Conversely, TCLs obtained from cells in which PLSCR1 is knocked-down associate with reduced DCs efficiency in eliciting antigen-specific T-cell-mediated immune responses. Although our results documented a functional role of PLSCR1 in these processes, further studies are needed to completely understand PLSCR1 modes of action. Regardless, the numerous studies describing PLSCR1 participation in anti-viral responses [26,29] have highlighted its contribution in IFN-induced innate immunity, whereas no information is currently available about its involvement in the regulation of cell-mediated adaptive responses. In the light of the results presented herein and of the contribution of PLSCR1 in plasmacytoid DC functions [49], it would be interesting to study a possible involvement of PLSCR1 in the adaptive immunity in the antiviral responses as well.

## Conclusions

Overall, our findings highlight the potential role of PLSCR1 in the regulation of immune responses during ICD and suggest that it may be a potential marker of immunogenicity in dying cancer cells. The ability of PLSCR1 to enhance this process could have important implications for the development of DC-based immunotherapies for cancer treatment.

## Declaration of Competing Interest

The authors have no commercial, proprietary or financial interest in the products or companies described in this article.

## CRedit authorship contribution statement

**Barbara Montico:** Conceptualization, Methodology, Investigation, Data curation, Writing – original draft. **Annunziata Nigro:** Methodology, Validation, Investigation, Data curation, Writing – original draft. **Maria Julia Lamberti:** Conceptualization, Software, Data curation, Writing – original draft. **Debora Martorelli:** Methodology, Validation. **Katy Mastorci:** Methodology. **Maria Ravo:** Methodology. **Giorgio Giurato:** Software. **Agostino Steffan:** Resources, Supervision. **Riccardo Dolcetti:** Resources, Writing – review & editing, Supervision. **Vincenzo Casolaro:** Software, Resources, Writing – review & editing, Supervision, Funding acquisition. **Jessica Dal Col:** Conceptualization, Validation, Investigation, Data curation, Writing – original draft, Funding acquisition.

## Funding

This research was funded by “AIRC Italian Association for Cancer Research” (My First Grant [MFAG 11729](#) to JDC),  $5 \times 1000$  Ministero della Salute Ricerca Corrente to A.S.; and [300397FRB19CASOL](#), [300397FRB21CASOL](#) to V.C.

## Acknowledgment

This study is based upon work from COST Action IMMUNO-model CA21135, supported by COST (European Cooperation in Science and Technology), <https://www.immuno-model.eu/>.

## Data Availability

Raw RNA sequencing data are deposited in the EBI ArrayExpress database (<http://www.ebi.ac.uk/arrayexpress>) with accession numbers E-MTAB-11799 and RNASeq table with the raw counts available in figshare (<https://doi.org/10.6084/m9.figshare.22283860>).

## Supplementary materials

Supplementary material associated with this article can be found in the online version at doi:[10.1016/j.jcyt.2023.11.014](https://doi.org/10.1016/j.jcyt.2023.11.014).

## References

- Garg AD, Dudek-Peric AM, Romano E, Agostinis P. Immunogenic cell death. *Int J Dev Biol* 2015;59:131–40.
- Kepp O, Senovilla L, Kroemer G. Immunogenic cell death inducers as anticancer agents. *Oncotarget* 2014;5:5190–1.
- Terenzi A, Pirker C, Keppler BK, Berger W. Anticancer metal drugs and immunogenic cell death. *J Inorg Biochem* 2016;165:71–9.
- Wang Q, Ju X, Wang J, Fan Y, Ren M, Zhang H. Immunogenic cell death in anticancer chemotherapy and its impact on clinical studies. *Cancer Lett* 2018;438:17–23.
- Zhou J, Wang C, Chen Y, Wang H, Hua Y, Cai Z. Immunogenic cell death in cancer therapy: present and emerging inducers. *J Cell Mol Med* 2019;23:4854–65.
- Liu P, Zhao L, Pol J, Levesque S, Petrazzuolo A, Pfirsche C, et al. Crizotinib-induced immunogenic cell death in non-small cell lung cancer. *Nat Commun* 2019;10:1486.
- Krysko DV, Garg AD, Kaczmarek A, Krysko O, Agostinis P, Vandenabeele P. Immunogenic cell death and DAMPs in cancer therapy. *Nat Rev Cancer* 2012;12:860–75.
- Rodrigues MC, Morais JAV, Ganassin R, Oliveira GRT, Costa FC, Morais AAC, et al. An overview on immunogenic cell death in cancer biology and therapy. *Pharmacetics* 2022;14.
- Garg AD, Nowis D, Golab J, Vandenabeele P, Krysko DV, Agostinis P. Immunogenic cell death, DAMPs and anticancer therapeutics: an emerging amalgamation. *Biochim Biophys Acta* 2010;1805:53–71.
- Garg AD, Nowis D, Golab J, Agostinis P. Photodynamic therapy: illuminating the road from cell death towards anti-tumour immunity. *Apoptosis* 2010;15:1050–71.
- Kroemer G, Galluzzi L, Kepp O, Zitvogel L. Immunogenic cell death in cancer therapy. *Annu Rev Immunol* 2013;31:51–72.
- Bloy N, Garcia P, Laumont CM, Pitt JM, Sistigu A, Stoll G, et al. Immunogenic stress and death of cancer cells: contribution of antigenicity vs adjuvanticity to immunosurveillance. *Immunol Rev* 2017;280:165–74.
- Lamberti MJ, Nigro A, Mentucci FM, Rumie Vittar NB, Casolaro V, Dal Col J. Dendritic cells and immunogenic cancer cell death: a combination for improving anti-tumor immunity. *Pharmaceutics* 2020;12.
- Montico B, Lapenta C, Ravo M, Martorelli D, Muraro E, Zeng B, et al. Exploiting a new strategy to induce immunogenic cell death to improve dendritic cell-based vaccines for lymphoma immunotherapy. *Oncoimmunology* 2017;6:e1356964.
- Decraene B, Yang Y, De Smet F, Garg AD, Agostinis P, De Vleeschouwer S. Immunogenic cell death and its therapeutic or prognostic potential in high-grade glioma. *Genes Immun* 2022;23:1–11.
- Liu Z, Xu X, Liu K, Zhang J, Ding D, Fu R. Immunogenic cell death in hematological malignancy therapy. *Adv Sci (Weinh)* 2023:e2207475.
- Sanchez-Paulete AR, Teijeira A, Cueto FJ, Garasa S, Perez-Gracia JL, Sanchez-Arrea A, et al. Antigen cross-presentation and T-cell cross-priming in cancer immunology and immunotherapy. *Ann Oncol* 2017;28(suppl. 12):xi44–55.
- Moriya T, Kitagawa K, Hayakawa Y, Hemmi H, Kaisho T, Ueha S, et al. Immunogenic tumor cell death promotes dendritic cell migration and inhibits tumor growth via enhanced T cell immunity. *iScience* 2021;24:102424.
- Garg AD, Martin S, Golab J, Agostinis P. Danger signalling during cancer cell death: origins, plasticity and regulation. *Cell Death Differ* 2014;21:26–38.
- Pozzi C, Cuomo A, Spadoni I, Magni E, Silvola A, Conte A, et al. The EGFR-specific antibody cetuximab combined with chemotherapy triggers immunogenic cell death. *Nat Med* 2016;22:624–31.
- Lamberti MJ, Mentucci FM, Roselli E, Araya P, Rivarola VA, Rumie Vittar NB, et al. Photodynamic modulation of type 1 interferon pathway on melanoma cells promotes dendritic cell activation. *Front Immunol* 2019;10:2614.
- Lamberti MJ, Montico B, Ravo M, Nigro A, Giurato G, Iorio R, et al. Integration of miRNA:mRNA co-expression revealed crucial mechanisms modulated in immunogenic cancer cell death. *Biomedicines* 2022;10.
- Mastorci K, Montico B, Fae DA, Sigalotti L, Ponzoni M, Inghirami G, et al. Phospholipid scramblase 1 as a critical node at the crossroad between autophagy and apoptosis in mantle cell lymphoma. *Oncotarget* 2016;7:41913–28.
- Herate C, Ramdani G, Grant NJ, Marion S, Gasman S, Niedergang F, et al. Phospholipid scramblase 1 modulates FcR-mediated phagocytosis in differentiated macrophages. *PLoS One* 2016;11:e0145617.
- Dal Col J, Lamberti MJ, Nigro A, Casolaro V, Fratta E, Steffan A, et al. Phospholipid scramblase 1: a protein with multiple functions via multiple molecular interactors. *Cell Commun Signal* 2022;20:78.
- Dong B, Zhou Q, Zhao J, Zhou A, Harty RN, Bose S, et al. Phospholipid scramblase 1 potentiates the antiviral activity of interferon. *J Virol* 2004;78:8983–93.
- Yang J, Zhu X, Liu J, Ding X, Han M, Hu W, et al. Inhibition of Hepatitis B virus replication by phospholipid scramblase 1 in vitro and in vivo. *Antiviral Res* 2012;94:9–17.
- Luo W, Zhang J, Liang L, Wang G, Li Q, Zhu P, et al. Phospholipid scramblase 1 interacts with influenza A virus NP, impairing its nuclear import and thereby suppressing virus replication. *PLoS Pathog* 2018;14:e1006851.
- Lizak M, Yarovinsky TO. Phospholipid scramblase 1 mediates type I interferon-induced protection against staphylococcal alpha-toxin. *Cell Host Microbe* 2012;11:70–80.
- George TC, Fanning SL, Fitzgerald-Bocarsly P, Medeiros RB, Highfill S, Shimizu Y, et al. Quantitative measurement of nuclear translocation events using similarity analysis of multispectral cellular images obtained in flow. *J Immunol Methods* 2006;311:117–29.
- Dal Col J, Mastorci K, Fae DA, Muraro E, Martorelli D, Inghirami G, et al. Retinoic acid/alpha-interferon combination inhibits growth and promotes apoptosis in mantle cell lymphoma through Akt-dependent modulation of critical targets. *Cancer Res* 2012;72:1825–35.
- Nigro A, Montico B, Casolaro V, Dal Col J. A novel dendritic cell-based vaccination protocol to stimulate immunosurveillance of aggressive cancers. *Methods Mol Biol* 2019;1884:317–33.
- Hashim A, Rizzo F, Marchese G, Ravo M, Tarallo R, Nassa G, et al. RNA sequencing identifies specific PIWI-interacting small non-coding RNA expression patterns in breast cancer. *Oncotarget* 2014;5:9901–10.
- Kim D, Perrea G, Trapnell C, Pimentel H, Kelley R, Salzberg SL. TopHat2: accurate alignment of transcriptomes in the presence of insertions, deletions and gene fusions. *Genome Biol* 2013;14:R36.
- Anders S, Huber W. Differential expression analysis for sequence count data. *Genome Biol* 2010;11:R106.
- Anders S, Pyl PT, Huber W. HTSeq—a Python framework to work with high-throughput sequencing data. *Bioinformatics* 2015;31:166–9.
- Goedhart J, Luijsterburg MS. VolcanoR is a web app for creating, exploring, labeling and sharing volcano plots. *Sci Rep* 2020;10:20560.

- [38] Subramanian A, Tamayo P, Mootha VK, Mukherjee S, Ebert BL, Gillette MA, et al. Gene set enrichment analysis: a knowledge-based approach for interpreting genome-wide expression profiles. *Proc Natl Acad Sci U S A* 2005;102:15545–50.
- [39] Garg AD, De Ruyscher D, Agostinis P. Immunological metagene signatures derived from immunogenic cancer cell death associate with improved survival of patients with lung, breast or ovarian malignancies: a large-scale meta-analysis. *Oncoimmunology* 2016;5:e1069938.
- [40] Mezzapelle R, Bianchi ME, Crippa MP. Immunogenic cell death and immunogenic surrender: related but distinct mechanisms of immune surveillance. *Cell Death Dis* 2021;12:869.
- [41] Rufo N, Korovesis D, Van Eygen S, Derua R, Garg AD, Finotello F, et al. Stress-induced inflammation evoked by immunogenic cell death is blunted by the IRE1-alpha kinase inhibitor KIRA6 through HSP60 targeting. *Cell Death Differ* 2022;29:230–45.
- [42] Heberle H, Meirelles GV, da Silva FR, Telles GP, Minghim R. InteractiVenn: a web-based tool for the analysis of sets through Venn diagrams. *BMC Bioinformatics* 2015;16:169.
- [43] Villanueva RAM, Chen ZJ. ggplot2: Elegant Graphics for Data Analysis (2nd ed.). Measurement: Interdisciplinary Research and Perspectives 2019;17:160–7.
- [44] Santini SM, Lapenta C, Logozzi M, Parlato S, Spada M, Di Pucchio T, et al. Type I interferon as a powerful adjuvant for monocyte-derived dendritic cell development and activity in vitro and in Hu-PBL-SCID mice. *J Exp Med* 2000;191:1777–88.
- [45] Lapenta C, Santini SM, Spada M, Donati S, Urbani F, Accapezzato D, et al. IFN-alpha-conditioned dendritic cells are highly efficient in inducing cross-priming CD8(+) T cells against exogenous viral antigens. *Eur J Immunol* 2006;36:2046–60.
- [46] Zhao KW, Li D, Zhao Q, Huang Y, Silverman RH, Sims PJ, et al. Interferon-alpha-induced expression of phospholipid scramblase 1 through STAT1 requires the sequential activation of protein kinase Cdelta and JNK. *J Biol Chem* 2005;280:42707–14.
- [47] Kodigepalli KM, Anur P, Spellman P, Sims PJ, Nanjundan M. Phospholipid scramblase 1, an interferon-regulated gene located at 3q23, is regulated by SnoN/SkiL in ovarian cancer cells. *Mol Cancer* 2013;12:32.
- [48] Vinnakota JM, Gummadi SN. Two c-Myc binding sites are crucial in upregulating the expression of human phospholipid scramblase 1 gene. *Biochem Biophys Res Commun* 2016;469:412–7.
- [49] Talukder AH, Bao M, Kim TW, Facchinetti V, Hanabuchi S, Bover L, et al. Phospholipid scramblase 1 regulates Toll-like receptor 9-mediated type I interferon production in plasmacytoid dendritic cells. *Cell Res* 2012;22:1129–39.
- [50] Ory S, Ceridono M, Momboisse F, Houy S, Chasserot-Golaz S, Heintz D, et al. Phospholipid scramblase-1-induced lipid reorganization regulates compensatory endocytosis in neuroendocrine cells. *J Neurosci* 2013;33:3545–56.
- [51] Sun J, Nanjundan M, Pike LJ, Wiedmer T, Sims PJ. Plasma membrane phospholipid scramblase 1 is enriched in lipid rafts and interacts with the epidermal growth factor receptor. *Biochemistry* 2002;41:6338–45.
- [52] Wiersma VR, Michalak M, Abdullah TM, Bremer E, Eggleton P. Mechanisms of translocation of ER chaperones to the cell surface and immunomodulatory roles in cancer and autoimmunity. *Front Oncol* 2015;5:7.
- [53] Krysko DV, Ravichandran KS, Vandenabeele P. Macrophages regulate the clearance of living cells by calreticulin. *Nat Commun* 2018;9:4644.
- [54] Lewinsky H, Gunes EG, David K, Radomir L, Kramer MP, Pellegrino B, et al. CD84 is a regulator of the immunosuppressive microenvironment in multiple myeloma. *JCI Insight* 2021;6.
- [55] Du H, Hirabayashi K, Ahn S, Kren NP, Montgomery SA, Wang X, et al. Antitumor responses in the absence of toxicity in solid tumors by targeting B7-H3 via chimeric antigen receptor T cells. *Cancer Cell* 2019;35:221–237.e8.
- [56] Spranger S, Gajewski TF. Tumor-intrinsic oncogene pathways mediating immune avoidance. *Oncoimmunology* 2016;5:e1086862.
- [57] Anderson NM, Simon MC. The tumor microenvironment. *Curr Biol* 2020;30:R921–R25.
- [58] Garg AD, More S, Rufo N, Mece O, Sassano ML, Agostinis P, et al. Trial watch: Immunogenic cell death induction by anticancer chemotherapeutics. *Oncoimmunology* 2017;6:e1386829.
- [59] Sistigu A, Yamazaki T, Vacchelli E, Chaba K, Enot DP, Adam J, et al. Cancer cell-autonomous contribution of type I interferon signaling to the efficacy of chemotherapy. *Nat Med* 2014;20:1301–9.
- [60] Vacchelli E, Sistigu A, Yamazaki T, Vitale I, Zitvogel L, Kroemer G. Autocrine signaling of type I interferons in successful anticancer chemotherapy. *Oncoimmunology* 2015;4:e988042.
- [61] Zitvogel L, Galluzzi L, Kepp O, Smyth MJ, Kroemer G. Type I interferons in anticancer immunity. *Nat Rev Immunol* 2015;15:405–14.
- [62] Der SD, Zhou A, Williams BR, Silverman RH. Identification of genes differentially regulated by interferon alpha, beta, or gamma using oligonucleotide arrays. *Proc Natl Acad Sci U S A* 1998;95:15623–8.
- [63] Zhou Q, Zhao J, Al-Zoghaibi F, Zhou A, Wiedmer T, Silverman RH, et al. Transcriptional control of the human plasma membrane phospholipid scramblase 1 gene is mediated by interferon-alpha. *Blood* 2000;95:2593–9.
- [64] Huang P, Liao R, Chen X, Wu X, Li X, Wang Y, et al. Nuclear translocation of PLSCR1 activates STAT1 signaling in basal-like breast cancer. *Theranostics* 2020;10:4644–58.
- [65] Li Y, Rogulski K, Zhou Q, Sims PJ, Prochownik EV. The negative c-Myc target onzin affects proliferation and apoptosis via its obligate interaction with phospholipid scramblase 1. *Mol Cell Biol* 2006;26:3401–13.
- [66] Bailey K, Cook HW, McMaster CR. The phospholipid scramblase PLSCR1 increases UV induced apoptosis primarily through the augmentation of the intrinsic apoptotic pathway and independent of direct phosphorylation by protein kinase C delta. *Biochim Biophys Acta* 2005;1733:199–209.
- [67] Frasch SC, Henson PM, Kailey JM, Richter DA, James MS, Fadok VA, et al. Regulation of phospholipid scramblase activity during apoptosis and cell activation by protein kinase Cdelta. *J Biol Chem* 2000;275:23065–73.
- [68] Kassas-Guediri A, Coudrat J, Pacreau E, Launay P, Monteiro RC, Blank U, et al. Phospholipid scramblase 1 amplifies anaphylactic reactions in vivo. *PLoS One* 2017;12:e0173815.
- [69] Pastorelli C, Veiga J, Charles N, Voignier E, Moussu H, Monteiro R, et al. Phospholipid scramblase, a new effector of FcepsilonRI signaling in mast cells. *Mol Immunol* 2002;38:1235–8.
- [70] Kassas A, Moura IC, Yamashita Y, Scheffel J, Guerin-Marchand C, Blank U, et al. Regulation of the tyrosine phosphorylation of Phospholipid Scramblase 1 in mast cells that are stimulated through the high-affinity IgE receptor. *PLoS One* 2014;9:e109800.
- [71] Tufail Y, Cook D, Fourgeaud L, Powers CJ, Merten K, Clark CL, et al. Phosphatidylserine exposure controls viral innate immune responses by microglia. *Neuron* 2017;93:574–86.e8.
- [72] Williamson P, Schlegel RA. Transbilayer phospholipid movement and the clearance of apoptotic cells. *Biochim Biophys Acta* 2002;1585:53–63.
- [73] Fadok VA, Bratton DL, Frasch SC, Warner ML, Henson PM. The role of phosphatidylserine in recognition of apoptotic cells by phagocytes. *Cell Death Differ* 1998;5:551–62.
- [74] Obeid M. ERP57 membrane translocation dictates the immunogenicity of tumor cell death by controlling the membrane translocation of calreticulin. *J Immunol* 2008;181:2533–43.
- [75] Kametaka S, Shibata M, Moroe K, Kanamori S, Ohsawa Y, Waguri S, et al. Identification of phospholipid scramblase 1 as a novel interacting molecule with beta-secretase (beta-site amyloid precursor protein (APP) cleaving enzyme (BACE)). *J Biol Chem* 2003;278:15239–45.
- [76] Ghiringhelli F, Apetoh L, Tesniere A, Aymeric L, Ma Y, Ortiz C, et al. Activation of the NLRP3 inflammasome in dendritic cells induces IL-1beta-dependent adaptive immunity against tumors. *Nat Med* 2009;15:1170–8.
- [77] Martin SJ. Cell death and inflammation: the case for IL-1 family cytokines as the canonical DAMPs of the immune system. *FEBS J* 2016;283:2599–615.
- [78] Anguille S, Smits EL, Lion E, van Tendeloo VF, Berneman ZN. Clinical use of dendritic cells for cancer therapy. *Lancet Oncol* 2014;15:e257–67.
- [79] Garg AD, Vandenberk L, Koks C, Verschuere T, Boon L, Van Gool SW, et al. Dendritic cell vaccines based on immunogenic cell death elicit danger signals and T cell-driven rejection of high-grade glioma. *Sci Transl Med* 2016;8:328ra27.
- [80] Carreno BM, Magrini V, Becker-Hapak M, Kaabinejadian S, Hundal J, Petti AA, et al. Cancer immunotherapy. A dendritic cell vaccine increases the breadth and diversity of melanoma neoantigen-specific T cells. *Science* 2015;348:803–8.
- [81] Storkus WJ, Maurer D, Lin Y, Ding F, Bose A, Lowe D, et al. Dendritic cell vaccines targeting tumor blood vessel antigens in combination with dasatinib induce therapeutic immune responses in patients with checkpoint-refractory advanced melanoma. *J Immunother Cancer* 2021;9.
- [82] Cox MC, Castiello L, Mattei M, Santodonato L, D'Agostino G, Muraro E, et al. Clinical and antitumor immune responses in relapsed/refractory follicular lymphoma patients after intranodal injections of IFNalpha-dendritic cells and rituximab: a phase I clinical trial. *Clin Cancer Res* 2019;25:5231–41.
- [83] Wculek SK, Cueto FJ, Mujal AM, Melero I, Krummel MF, Sancho D. Dendritic cells in cancer immunology and immunotherapy. *Nat Rev Immunol* 2020;20:7–24.
- [84] Thara E, Dorff TB, Pinski JK, Quinn DI. Vaccine therapy with sipuleucel-T (Provenge) for prostate cancer. *Maturitas* 2011;69:296–303.
- [85] Fucikova J, Moserova I, Truxova I, Hermanova I, Vancurova I, Partlova S, et al. High hydrostatic pressure induces immunogenic cell death in human tumor cells. *Int J Cancer* 2014;135:1165–77.
- [86] Montico B, Nigro A, Casolaro V, Dal Col J. Immunogenic apoptosis as a novel tool for anticancer vaccine development. *Int J Mol Sci* 2018;19.